J. Fluid Mech. (1978), *vol.* 87, *part* 1, *pp.* 65–84
Printed in Great Britain

On the stability of thermally driven shear flow heated from below

By J. E. WEBER
The Norwegian Meteorological Institute, Blindern, Oslo 3, Norway

(Received 9 May 1977 and in revised form 19 December 1977)

The onset of convection in shear flow driven by lateral heating and also uniformly heated from below is investigated numerically by Galerkin's method. Stress-free as well as rigid, perfectly conducting boundaries are considered. The analysis is valid for small and moderate Prandtl numbers. The magnitude of the lateral basic temperature gradient may be expressed by a dimensionless Grashof number G, while the uniform heating from below is represented by a Rayleigh number Ra. Depending on the values of G, Ra and the Prandtl number Pr, a variety of interesting situations arise. In particular it is demonstrated that the form of the most unstable mode, i.e. whether it is a roll with axis aligned along the basic flow (a longitudinal roll) or one with axis normal to the basic flow (a transverse roll), depends on the value of the Prandtl number. For small values of G, the marginally stable disturbances are found to be steady, while for larger values of G, oscillatory instability occurs. For all values of G considered here ($G \lesssim 3000$), computations of the energy balance for the marginally stable disturbances show that the main instability mechanism is of thermal origin, while the effect of shear may be important in selecting the preferred mode of disturbance.

1. Introduction

The stability of thermally driven shear flow has not attracted much attention in the literature, despite the variety of geophysical and technical problems in which this type of flow occurs; see the recent review by Kelly (1977). The basic flow itself, in its simplest form, is governed by a balance between vorticity due to horizontal density variations, and viscous diffusion of vorticity. Large-scale turbulent analogues in Nature include the atmospheric 'sea breeze' (Walsh 1974; Neuman & Mahrer 1974) and flows in estuaries and coastal waters caused by the discharge of pollutants from urban districts or waste water from nuclear or fossil electric power generation (Cormack, Stone & Leal 1975).

Hart (1972) investigated theoretically the stability of this kind of circulation (sometimes called a Hadley circulation in meteorology) on the assumption that the ratio of the height to the length was small. The existence of such a basic flow was demonstrated experimentally by Imberger (1974), who found that the flow in the central part of a side-heated shallow container was approximately rectilinear with a constant horizontal temperature gradient. From his stability analysis, Hart (1972) found that, for sufficiently large values of the non-dimensional horizontal temperature gradient, instability would occur in the form of two-dimensional disturbances with

axes normal to the basic flow (transverse rolls) for all values of the Prandtl number. Hurle, Jakeman & Johnson (1974), on the other hand, observed longitudinal oscillatory rolls (rolls with axes aligned with the flow) in a side-heated container filled with a low Prandtl number fluid. In the latter case, however, the geometry of the model is likely to have affected the selection of mode, and also the measurement technique may not have been sensitive enough to detect transverse disturbances; see the discussion by Gill (1974) on this and related experiments.

Some effects of horizontal non-uniform heating were demonstrated experimentally by Koschmieder (1966) in a shallow cylindrical container whose upper boundary was held at a constant temperature while the lower had a radial temperature gradient. Under subcritical conditions one large roll was observed but this broke up into axially symmetric rolls of different sizes and circulations when the vertical temperature difference was sufficiently increased. A closely similar experiment in a rectangular cavity has been reported by Berkovsky & Fertman (1970).

Weber (1973) separated the effects of side heating and uniform heating from below by assuming that equal and constant temperature gradients existed along both boundaries of a shallow, horizontal fluid layer (cf. Hart 1972) but that the vertical temperature difference was non-zero. By taking the horizontal gradient to be small, it was shown analytically that the resulting thermally driven shear flow stabilized the Rayleigh–Bénard convection problem for stress-free and perfectly conducting boundaries. In particular it was demonstrated that the preferred mode of disturbance depended crucially on the Prandtl number.

In the present paper we follow Weber (1973, hereafter referred to as I) and consider the general linear stability problem for stress-free as well as rigid (no-slip) boundary conditions. It should be emphasized that the assumptions behind this model differ from the experimental conditions of Koschmieder (1966) and Berkovsky & Fertman (1970). In particular, our vertical temperature gradient is independent of the lateral co-ordinate, while this is not so in the cited experiments. This makes direct comparison inappropriate. In fact, a completely suitable experiment may be difficult to design, especially for large values of G.

Three independent parameters define the stability problem: a Prandtl number, a vertical Rayleigh number and a horizontal Grashof number (the aspect ratio = depth/width is assumed to be zero). The marginally stable solutions, in which the horizontal wavenumbers are taken to be those which minimize the Rayleigh number, will then be confined to a surface in a three-dimensional parameter space. This means that a complete analysis of the linear stability problem would require vast amounts of computer time. To restrict the problem we have approached it by investigating how an increasingly stronger horizontal temperature gradient modifies the ordinary Rayleigh–Bénard problem. The Prandtl number is allowed to vary from zero to about ten, covering most values encountered in geophysical or astrophysical fluid dynamics (when defined in terms of the molecular or customarily chosen eddy coefficients).

The Prandtl number again turns out to have a very interesting effect on the stability problem, particularly in determining the form of the fastest-growing disturbances.

Besides calculating the stability curves we have also considered the energy balance for the marginally stable solutions. It is shown that this in some cases may provide a clue to the reason why a certain type of disturbance is preferred.

2. Basic flow

The basic model to be investigated is the same as in I. The fluid is confined between horizontal planes a distance d apart. A Cartesian co-ordinate system (x, y, z) is chosen such that the y axis is vertical with origin in the middle of the layer. The lateral temperature variation along the boundaries is taken to be linear in the x direction. For a given value of x, the temperature difference ΔT between the planes is constant. We may thus write

$$T = T_0 - \tfrac{1}{2}\Delta T - \beta x, \quad T = T_0 + \tfrac{1}{2}\Delta T - \beta x$$

at the top and bottom plane, respectively, where β is a positive constant. The ratio of the height to the length of the model is assumed to be so small that lateral end effects do not affect the motion in the central part, i.e. the model is taken to be of infinite horizontal extent.

Contrary to I, we now choose a non-dimensionalization which is appropriate for small and moderate Prandtl numbers. This is achieved by taking

$$\nu/d, \quad d^2/\nu, \quad \rho_0 \nu^2/d^2, \quad \nu^2/g\gamma d^3 \tag{2.1}$$

as units for the velocity $\mathbf{v}\,[=(u, v, w)]$, time t, pressure p and temperature T. In (2.1), ν is the kinematic viscosity and γ the thermal coefficient of expansion. By making the Boussinesq approximation, the non-dimensional governing equations may be written as

$$\partial \mathbf{v}/\partial t + \mathbf{v}.\nabla \mathbf{v} = -\nabla p + \nabla^2 \mathbf{v} + T\mathbf{j}, \tag{2.2}$$

$$Pr(\partial T/\partial t + \mathbf{v}.\nabla T) = \nabla^2 T, \tag{2.3}$$

$$\nabla.\mathbf{v} = 0, \tag{2.4}$$

where $\mathbf{j}$ is a vertical unit vector and $Pr = \nu/\kappa$ is the Prandtl number, in which κ is the thermal diffusivity.

In analogy with Hart (1972) or I, a basic solution is obtained by assuming

$$\left.\begin{aligned} \partial/\partial t = v = w = 0, \\ u = U(y), \quad T = T(y) - Gx, \end{aligned}\right\} \tag{2.5}$$

where G is a horizontal Grashof number defined by $G = g\gamma\beta d^4/\nu^2$.

For stress-free boundaries, we obtain

$$\left.\begin{aligned} U(y) &= \tfrac{1}{2}G(\tfrac{1}{4}y - \tfrac{1}{3}y^3), \\ T(y) &= \tfrac{1}{24} Pr\, G^2(\tfrac{9}{80}y - \tfrac{1}{2}y^3 + \tfrac{1}{5}y^5) - \tilde{G}y, \end{aligned}\right\} \tag{2.6}$$

where $\tilde{G}$ $(=g\gamma\Delta T d^3/\nu^2)$ is a vertical Grashof number.

For rigid (i.e. no-slip) boundaries, the equations yield

$$\left.\begin{aligned} U(y) &= \tfrac{1}{6}G(\tfrac{1}{4}y - y^3), \\ T(y) &= \tfrac{1}{24} Pr\, G^2(\tfrac{7}{240}y - \tfrac{1}{6}y^3 + \tfrac{1}{5}y^5) - \tilde{G}y. \end{aligned}\right\} \tag{2.7}$$

In both cases the boundaries have been assumed to be perfectly conducting.

It should be noted, however, that in many practical cases, as in the laboratory, the finite length l of the model will impose restrictions on the validity of the solutions (2.6) and (2.7). Since the vertical temperature difference due to side heating can never exceed the temperature difference between the vertical end walls, one finds

$$PrG \leqslant O(1000l/d), \tag{2.8}$$

while Hart (1972) reports from measurements that the basic parallel type of flow exists provided that

$$G \lesssim 800l/d. \tag{2.9}$$

3. Stability analysis

On perturbing the governing equations through infinitesimal disturbances of the form $f(y)\exp\{ikx+imz+\omega t\}$, where $f(y)$ is in general complex, k and m are real wavenumbers in the x and z directions, respectively, and ω is the complex growth rate, we finally obtain

$$(D^2-\alpha^2-ikGU_*-\omega)(D^2-\alpha^2)v+ikGD^2U_*v-\alpha^2\theta=0, \tag{3.1}$$

$$(D^2-\alpha^2-ikPrGU_*-Pr\omega)\theta+PrGu+Rav-Pr^2G^2D\Theta_*v=0, \tag{3.2}$$

$$(D^2-\alpha^2-ikGU_*-\omega)(-\alpha^2u+ikDv)+m^2GDU_*v=0, \tag{3.3}$$

where $D=d/dy$, u, v and θ are the y-dependent parts of the velocity and temperature perturbations, $Ra\equiv Pr\tilde{G}=g\gamma\Delta Td^3/\nu\kappa$ is the Rayleigh number and $\alpha=(k^2+m^2)^{\frac{1}{2}}$ is the horizontal overall wavenumber. Furthermore we have defined

$$U_*\equiv U(y)/G, \quad \Theta_*\equiv T(y)/PrG^2+\tilde{G}y/PrG^2. \tag{3.4}$$

Equations (3.1)–(3.3) are subject to the boundary conditions

$$v=D^2v=Du=\theta=0 \quad \text{at} \quad y=\pm\tfrac{1}{2} \tag{3.5}$$

in the free case, while rigid boundaries require

$$v=Dv=u=\theta=0 \quad \text{at} \quad y=\pm\tfrac{1}{2}. \tag{3.6}$$

In I, with a different non-dimensionalization, the equivalent system of equations was solved for stress-free boundaries by a perturbation technique, under the assumption of a small horizontal temperature variation. The analysis was simplified by approximating the exact profiles of U_* and Θ_* by trigonometric expressions. However, this approximation is not essential. With the exact values of U_* and Θ_* we obtain closely similar results; see appendix A.

For larger values of the parameter G in the free case and in general for rigid boundaries, the stability problem must be solved numerically. Galerkin's method proves adequate for this purpose. The set of ordinary differential equations (3.1)–(3.3) is converted into a matrix eigenvalue problem for the eigenvalues ω. The variables are expanded in N-term expansions in eigenfunctions satisfying the appropriate boundary conditions. Accordingly

$$v=\Sigma a_iX_i, \quad \theta=\Sigma b_iY_i, \quad u=\Sigma c_iZ_i, \tag{3.7}$$

where

$$X_i=D^2X_i=Y_i=DZ_i=0 \quad \text{at} \quad y=\pm\tfrac{1}{2} \tag{3.8}$$

if the boundaries are taken to be stress-free and

$$X_i = DX_i = Y_i = Z_i = 0 \quad \text{at} \quad y = \pm \tfrac{1}{2} \tag{3.9}$$

in the rigid case.

For free boundaries trigonometric functions were chosen as expansion functions, while polynomials were chosen in the rigid case; see Finlayson (1972, p. 154) and also appendix B of the present paper. Since the computations in I showed that the most unstable disturbances were two-dimensional with axes either normal to the basic flow (transverse rolls) or aligned with the basic flow (longitudinal rolls), we have concentrated on these two modes in the numerical computations. This seems also to be supported, for rigid boundaries, by the experimental results of Koschmieder (1966) and Berkovsky & Fertman (1970), although these may not be directly relevant to the present problem. We take the view that, in the absence of any experimental evidence suggesting three-dimensionality of the fastest-growing disturbances, a three-dimensional numerical study is not as yet justified.

By eliminating u from (3.1)–(3.3) the transverse problem gives rise to a $2N \times 2N$ matrix equation with complex coefficients. Owing to the antisymmetry of the basic flow, however, a simple transformation may be introduced which renders all the coefficients real except the complex eigenvalue; see Gallagher & Mercer (1965) or Hart (1970) for details.

The longitudinal problem separates into non-combining even and odd modes, as may easily be seen from (3.1)–(3.3). Hence a reduction from one $3N \times 3N$ matrix equation to two $\frac{3}{2}N \times \frac{3}{2}N$ matrix equations is achieved (with N chosen as an even number). N was chosen large enough that $|\omega_{N+2} - \omega_N|/|\omega_N| \ll 1$ and also such that the average energy equations balanced (see the next section), although this was not a very sensitive test. The convergence was found to depend very much on the Prandtl number and two examples are given in appendix B, tables 5 and 6. For most computations we used 14 and 7 terms in the expansions for the transverse and longitudinal problems respectively.

4. Energy considerations

Some understanding of the nature of the stability problem may be gained by looking at the energy balance for the perturbations. We insert the perturbed velocity and temperature fields into (2.2) and take the real part. By multiplying by the real part of the perturbation velocity, averaging over a wavelength in the x and z directions, integrating from $y = -\frac{1}{2}$ to $y = +\frac{1}{2}$ and using the boundary conditions, one obtains the familiar equation for the kinetic energy of the perturbation.

For the special case of longitudinal rolls ($\partial/\partial x = 0$), the equation splits up into

$$\partial(\tfrac{1}{2}\langle \overline{u^2} \rangle)/\partial t = -G\langle DU_* \overline{uv} \rangle - \langle \overline{\nabla u^2} \rangle \tag{4.1}$$

and

$$\partial(\tfrac{1}{2}\langle \overline{v^2 + w^2} \rangle)/\partial t = \langle \overline{v\theta} \rangle - \langle \overline{\nabla v^2} + \overline{\nabla w^2} \rangle, \tag{4.2}$$

while for transverse rolls ($\partial/\partial z = 0$), the equation reduces to

$$\partial(\tfrac{1}{2}\langle \overline{w^2} \rangle)/\partial t = -\langle \overline{\nabla w^2} \rangle, \quad \text{i.e.} \quad w \to 0, \tag{4.3}$$

and $$\partial(\tfrac{1}{2}\langle\overline{u}^2+\overline{v}^2\rangle)/\partial t = -G\langle DU_*\,\overline{uv}\rangle + \langle\overline{v\theta}\rangle - \langle\overline{\nabla u}^2+\overline{\nabla v}^2\rangle, \tag{4.4}$$

or $$\partial I_0/\partial t = I_1+I_2+I_3.$$

Here the bars and brackets denote horizontal means and vertical integrations respectively.

Some well-known results may be deduced from these equations. For convection in the form of longitudinal rolls in a shear flow which is *not* thermally driven (e.g. Couette/Poiseuille flow), the pressure does not couple the horizontal perturbation velocity u to the stability problem, i.e. a longitudinal roll does not 'feel' the effect of shear, and accordingly any instability must be of thermal origin.† For given v and θ then, u can in principle be determined from the x component of the momentum equation. Energetically, it is seen from (4.1) that for marginally stable solutions the u component is sustained by extracting energy from the basic flow.

For transverse rolls the presence of shear may be stabilizing or destabilizing. The instability is said to be of hydrodynamic origin (shear instability) if $I_1 \gg I_2$ and of convective (thermal) origin if $I_1 \ll I_2$. It is important to note that, even if the basic instability mechanism is thermal, the preferred mode of disturbance may depend crucially on the shear. Since longitudinal rolls are not affected by shear, the sign of I_1 for transverse rolls will be decisive. If $I_1 > 0$, i.e. transverse rolls extract energy from the basic flow, this type of disturbance will be preferred, while for $I_1 < 0$, as for convection in Couette flow (Asai 1970), longitudinal rolls will occur.

In the present problem, where the basic temperature field varies in the horizontal as well in the vertical, u, v and θ are all coupled for longitudinal rolls, as may be seen from (3.1)–(3.3). To get an idea of the strength of this coupling we consider the balance for the square of the perturbation temperature. By taking the real part of (3.2), multiplying by $\mathscr{R}\theta$ and averaging and integrating as before, we obtain

$$Pr\,\partial(\langle\tfrac{1}{2}\overline{\theta^2}\rangle)/\partial t = Pr\,G\langle\overline{u\theta}\rangle + Ra\langle\overline{v\theta}\rangle - Pr^2\,G^2\langle D\Theta_*\,\overline{v\theta}\rangle - \langle(\overline{\nabla\theta})^2\rangle, \tag{4.5}$$

or $$\partial T_0/\partial t = T_1+T_2+T_3+T_4.$$

The first term on the right, T_1, arises from the horizontal basic temperature gradient and may in certain cases provide a source of buoyancy. T_2 is proportional to the conversion of potential energy from the linear part of the vertical temperature variation, as in the ordinary Rayleigh–Bénard problem, while T_3 arises from the vertical temperature distribution associated with the Hadley circulation. Since $D\Theta_*$ is negative near the boundaries and positive in the middle of the layer, this term may be stabilizing or destabilizing. It should be noted that in the case of insulating boundaries $D\Theta_* \geqslant 0$ everywhere, and therefore this term does not contribute to instability. The last term in (4.5), T_4, is always stabilizing, and may conveniently be termed thermal dissipation.

Since the temperature in (3.2) represents buoyancy, the physics behind (4.5) is quite similar to that behind (4.4), except that no shear effect is present and viscous dissipation is replaced by thermal dissipation. These equations will both be referred to as energy equations.

† If nonlinear effects are included, however, the development of a longitudinal roll and the associated growth of the u component in turn change the total basic velocity profile, so that this may become unstable to transverse disturbances; see Ellingsen & Palm (1975) for a discusson of the inviscid case.

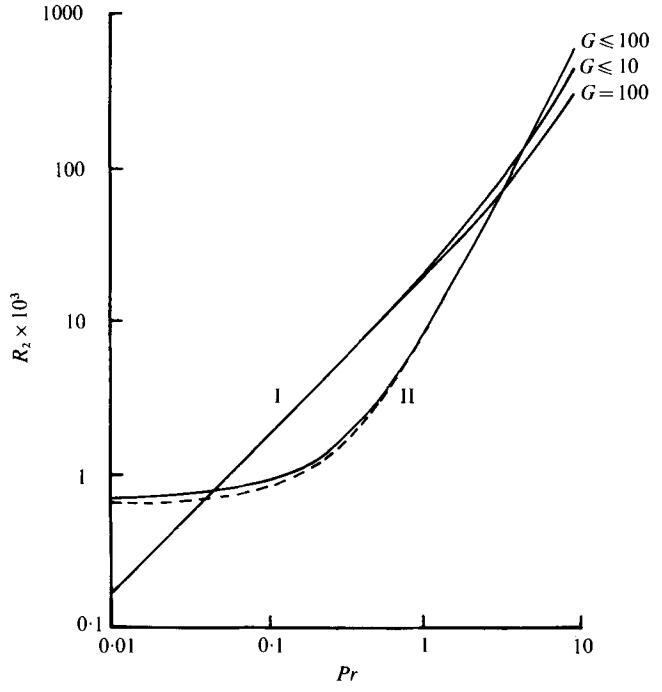

FIGURE 1. $R_2 = (Ra^c - R_0)/G^2$ *vs. Pr* for free boundaries and $G \leqslant 100$. I, longitudinal steady rolls (even mode); II, transverse steady rolls. The broken line for transverse rolls represents the analytical result (A 2), while the analytical result for longitudinal rolls is indistinguishable from the numerical one for $G \leqslant 10$.

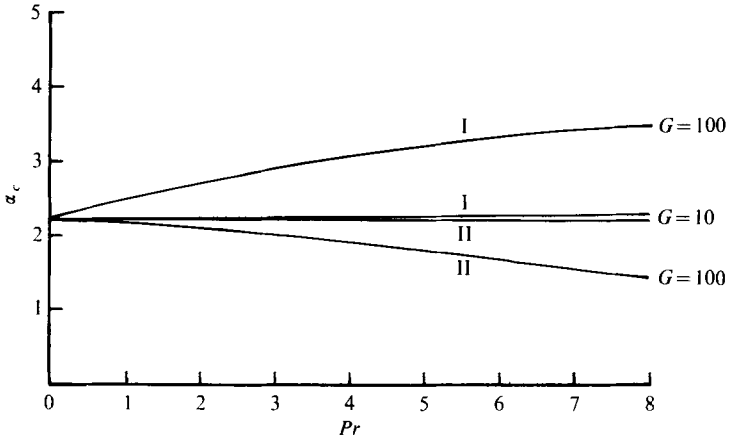

FIGURE 2. Critical wavenumber *vs.* Prandtl number for free boundaries and $G \leqslant 100$. I, longitudinal rolls; II, transverse rolls.

Pr	$I_1 \times 10^2$	$I_2 \times 10^2$	$I_3 \times 10^2$	T_1	T_2	T_3	T_4
0·01	−0·005	0·557	−0·552	0·0001	3·6998	−0	−3·6999
0·1	−0·005	0·556	−0·551	0·0025	3·7037	−0·0015	−3·7046
1	−0·011	0·553	−0·542	0·138	4·046	−0·152	−4·032
10	−0·011	0·197	−0·186	5·272	12·705	−5·509	−12·468

TABLE 1. Energy balance at $G = 100$ for marginally stable transverse rolls and free boundaries.

Pr	T_1	T_2	T_3	T_4
0·01	−0·0097	3·7092	−0	−3·6995
0·1	−0·0927	3·8842	−0·0016	−3·7899
1	−0·8239	5·0203	−0·1659	−4·0304
10	−4·53	26·98	−9·48	−12·96

TABLE 2. Thermal balance at $G = 100$ for marginally stable longitudinal rolls (even modes) and free boundaries.

5. Numerical results

Free boundaries

Some of the results are presented in figures 1–5. It proves convenient, at least for small values of G, to define the quantity $R_2 \equiv (Ra^c - R_0)/G^2$, where R_0 is the critical Rayleigh number for convection in the absence of shear. It is then easy to compare the numerical and analytical results, since, for sufficiently small G, R_2 will be independent of G and vary with the Prandtl number only.

In figure 1 results for free boundaries have been plotted for various values of $G \leqslant 100$. The computations showed that, for a given value of Pr, for longitudinal rolls R_2 was practically unchanged when G was increased up to 10, while for transverse rolls R_2 was constant up to about $G = 100$. For $G \lesssim 10$, the figure shows that the numerical results differ very little from the analytical expression (A 2). Since the most unstable linear perturbation, i.e. the one that corresponds to the smallest critical Rayleigh number, is expected to dominate the motion at slightly supercritical Rayleigh numbers also, suppressing the growth of other unstable modes, we conclude that for values of G up to about 10 transverse rolls will be preferred when $0{\cdot}04 < Pr < 5{\cdot}2$, while longitudinal rolls will occur outside this range. For larger values of G, R_2 increases less rapidly with Pr for longitudinal rolls, as demonstrated by the curve for $G = 100$. Hence the transverse region tends to decrease, and at $G = 100$ longitudinal rolls take over for $Pr \gtrsim 3{\cdot}7$. Further, the computations showed that the marginally stable disturbances did not propagate relative to the boundaries, and it was found that the even longitudinal mode was always more unstable than the odd mode.

In figure 2 we have displayed the critical wavenumber as a function of the Prandtl number for $G = 10$ and $G = 100$. The results show a marked tendency towards an increase in wavelength for transverse rolls for increasing Pr and G, while the wavelength for the longitudinal modes decreases.

We have also calculated the energy balances (4.4) and (4.5) for the marginally stable solutions. The results presented in tables 1 and 2 have been obtained for $G = 100$.

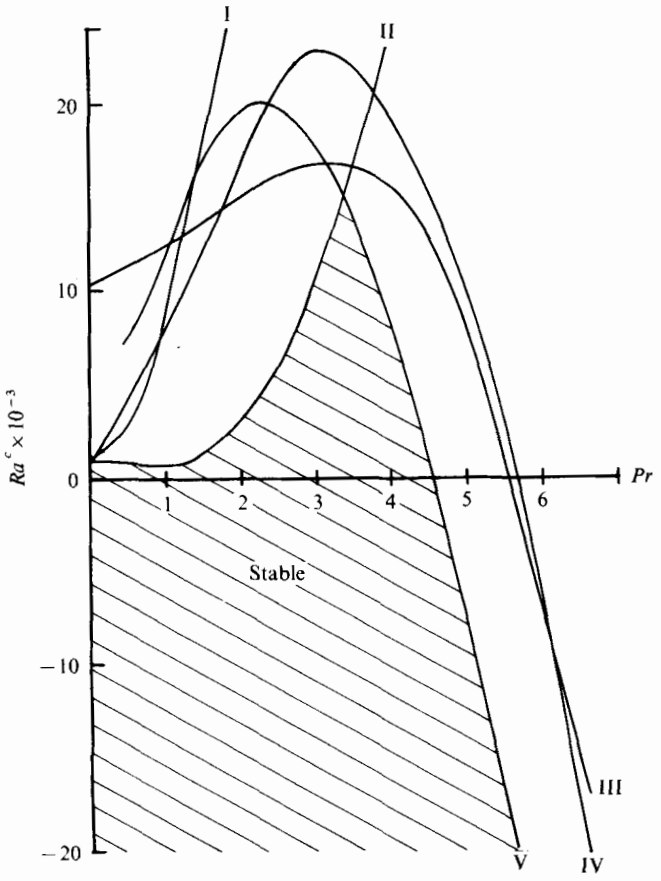

FIGURE 3. Critical Rayleigh number *vs.* Prandtl number for free boundaries and $G = 1000$. I, transverse steady rolls; II, longitudinal oscillatory rolls (even mode); III, longitudinal steady rolls (odd mode); IV, longitudinal steady rolls (even mode); V, transverse oscillatory rolls.

For longitudinal rolls the shear effect formally decouples from the buoyancy as far as the kinetic energy is concerned. This makes the numerical values of the balancing terms in (4.1) and (4.2) rather insignificant, and they will not be stated here. The balance in (4.5), however, yields the values given in table 2.

The first thing to note from tables 1 and 2 is that $I_1 = -G\langle DU_* \overline{uv}\rangle$ is negative, i.e. transverse rolls always lose energy to the basic flow through the shear mechanism. We further observe that the term $T_3 = -Pr^2G^2\langle D\Theta_* \overline{v\theta}\rangle$ in the thermal balance is stabilizing for transverse as well as longitudinal rolls, which means that for this value of G the Hadley circulation just brings warm fluid above cold fluid and thus stabilizes the layer in the vertical. We note that the potential energy term $T_1 = Pr\,G\langle\overline{u\theta}\rangle$ always acts in a destabilizing sense for transverse rolls but is stabilizing for longitudinal rolls. For some Prandtl numbers this destabilizing effect seems to override any stabilizing tendency caused by the shear, which may explain why transverse rolls occur in a certain range of Prandtl numbers.

It is also obvious why longitudinal rolls are preferred for sufficiently small Prandtl numbers in the free case. In the limit $Pr = 0$ the temperature equation (3.2) reduces

to that of ordinary convection without shear. Also, for longitudinal rolls with $k \equiv 0$, the shear term in the momentum equation (3.1) vanishes. Accordingly the critical Rayleigh number will be the same as for ordinary convection, i.e.

$$Ra^c_{\text{long}} = R_0 = \tfrac{27}{4}\pi^4.$$

For transverse rolls in the limit $Pr = 0$ the shear effect is still stabilizing, and accordingly $Ra^c_{\text{trans}} > R_0$.

For larger values of G the stability picture becomes more complicated. As an example we have considered $G = 1000$; see figure 3. Since by definition

$$G \equiv g\gamma\beta d^4/\nu^2 \equiv \left(\frac{\beta}{\Delta T/d}\right) Ra\, Pr^{-1},$$

we see that for a Prandtl number of order unity the horizontal and vertical temperature gradients would be of the same order of magnitude if instability began at the critical Rayleigh number corresponding to ordinary Rayleigh–Bénard convection.

Oscillatory modes will now be the most unstable ones. For $Pr < 3{\cdot}4$ a longitudinal oscillatory even mode will be preferred, and we note that the critical Rayleigh number has a local minimum near $Pr = 1$ where $0 < Ra^c < R_0$. At this point the various terms in the thermal balance (4.5) have the following values:

$$T_1 = 4{\cdot}584, \quad T_2 = 0{\cdot}369, \quad T_3 = -1{\cdot}140, \quad T_4 = -3{\cdot}813. \tag{5.1}$$

We observe that $T_1 = Pr\, G\langle\overline{u\theta}\rangle$ is the dominating destabilizing term, which means that the horizontal temperature gradient in this case provides a sufficient source of buoyancy for convection to occur.

For $Pr > 3{\cdot}4$ it is seen that transverse oscillatory rolls will take over, and for $Pr > 4{\cdot}55$ instability will occur even if the layer is uniformly heated from the top, i.e. when $Ra < 0$. If we choose $Pr = 5$ the terms in the energy balances (4.4) and (4.5) turn out to be

$$I_1 = 0{\cdot}004 \times 10^{-2}, \quad I_2 = 0{\cdot}149 \times 10^{-2}, \quad I_3 = -0{\cdot}153 \times 10^{-2} \tag{5.2}$$

and

$$T_1 = 0{\cdot}3, \quad T_2 = -11{\cdot}4, \quad T_3 = 130{\cdot}9, \quad T_4 = -119{\cdot}8. \tag{5.3}$$

Since here $I_1 \ll I_2$, the instability is of thermal origin. From the thermal balance we observe that the dominant destabilizing term is $T_3 = -Pr^2 G^2\langle D\Theta_* \overline{v\theta}\rangle$, implying that instability now arises from the vertical temperature distribution associated with the Hadley circulation.

Equivalently, we may define a lateral Rayleigh number $Ra_L \equiv Pr\, G$. From figure 3 we then find that when the vertical Rayleigh number Ra is zero transverse oscillatory rolls will become unstable when $Ra_L \geqslant 4550$.

In figure 4 we have plotted the critical wavenumbers for the marginally stable modes. The decrease in wavelength for unstable transverse oscillatory rolls when $Pr > 3{\cdot}5$ again emphasizes the fact that the main source of buoyancy is not uniformly distributed throughout the layer, but confined to certain parts. In figure 5 we have plotted the phase speed for marginally stable disturbances. For comparison we have also displayed the maximum speed of the basic flow for $G = 1000$, and it is seen that the disturbances always travel with a velocity less than $U_{\max}$.

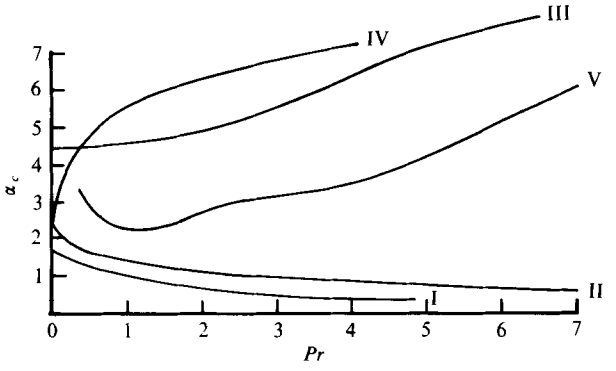

FIGURE 4. Critical wavenumber *vs.* Prandtl number for free boundaries and $G = 1000$. Curves as in figure 3.

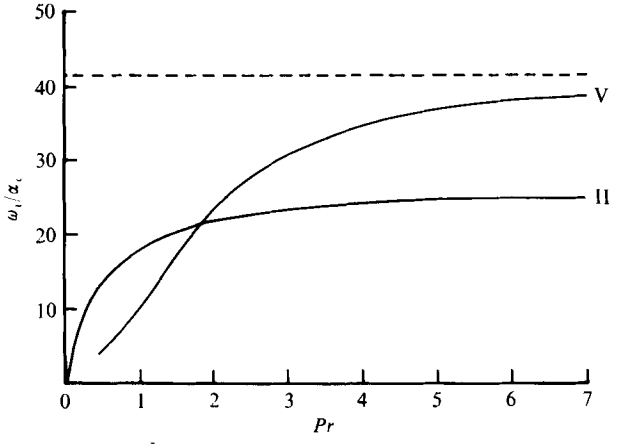

FIGURE 5. Phase speed *vs.* Prandtl number for the marginally stable oscillatory modes displayed in figure 4. V, transverse rolls; II, longitudinal rolls (even mode). The broken line at the top represents the maximum speed of the basic flow.

Rigid boundaries

Some results for rigid boundaries are shown in figures 6–11. No significant change in $R_2 \equiv (Ra^c - R_0)/G^2$ was found for $G \leqslant 100$ for either type of disturbance. From figure 6 we observe that transverse rolls now occur for *all* Prandtl numbers less than 1·75 when $G \leqslant 100$, while longitudinal rolls take over when $Pr > 1{\cdot}75$. Up to $G = 100$ the critical wavenumbers were not found to vary much with increasing Pr and G, but there was still a slight tendency towards an increase in wavelength for transverse rolls and a decrease for longitudinal rolls.

In tables 3 and 4 we have displayed the values of the various terms in the energy balances for the marginally stable solutions at $G = 100$.

We observe from table 3 that $I_1 > 0$ when Pr is small, i.e. shear now has a destabilizing effect on transverse rolls. In figure 7 we have plotted R_2 as a function of Pr in this region. For small values of Pr, R_2 did not vary significantly with G for $G \leqslant 1000$, and we find that $R_2 < 0$, i.e. $Ra^c < R_0$, when $Pr \leqslant 0{\cdot}12$.

Pr	$I_1 \times 10^2$	$I_2 \times 10^2$	$I_3 \times 10^2$	T_1	T_2	T_3	T_4
0·01	0·0002	0·5123	−0·5125	−0	8·7473	−0	−8·7473
0·1	0·0002	0·5122	−0·5124	0·0001	8·7480	−0·0004	−8·7477
1	−0·0002	0·5117	−0·5115	0·0365	8·8208	−0·0381	−8·8192
10	−0·0034	0·4656	−0·4622	3·62	15·22	−3·45	−15·39

TABLE 3. Energy balances at $G = 100$ for marginally stable transverse rolls and rigid boundaries.

Pr	T_1	T_2	T_3	T_4
0·01	−0·0007	8·7479	−0	−8·7472
0·1	−0·0074	8·7550	−0·0004	−8·7472
1	−0·0739	8·8679	−0·0381	−8·7559
10	0·817	15·112	−4·168	−10·127

TABLE 4. Thermal balance at $G = 100$ for marginally stable longitudinal rolls (even mode) and rigid boundaries.

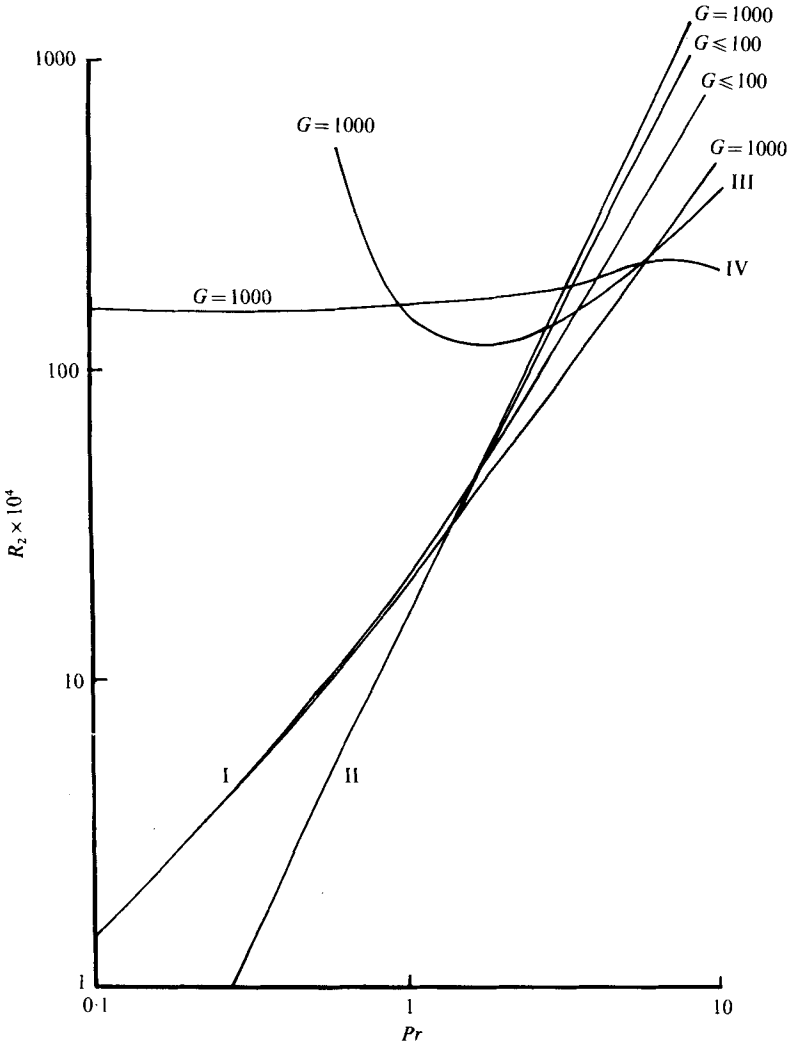

FIGURE 6. $R_2 = (Ra^c - R_0)/G^2$ *vs.* Pr for rigid boundaries and $G \leqslant 1000$. I, longitudinal steady rolls (even mode); II, transverse steady rolls; III, transverse oscillatory rolls; IV, longitudinal steady rolls (odd mode).

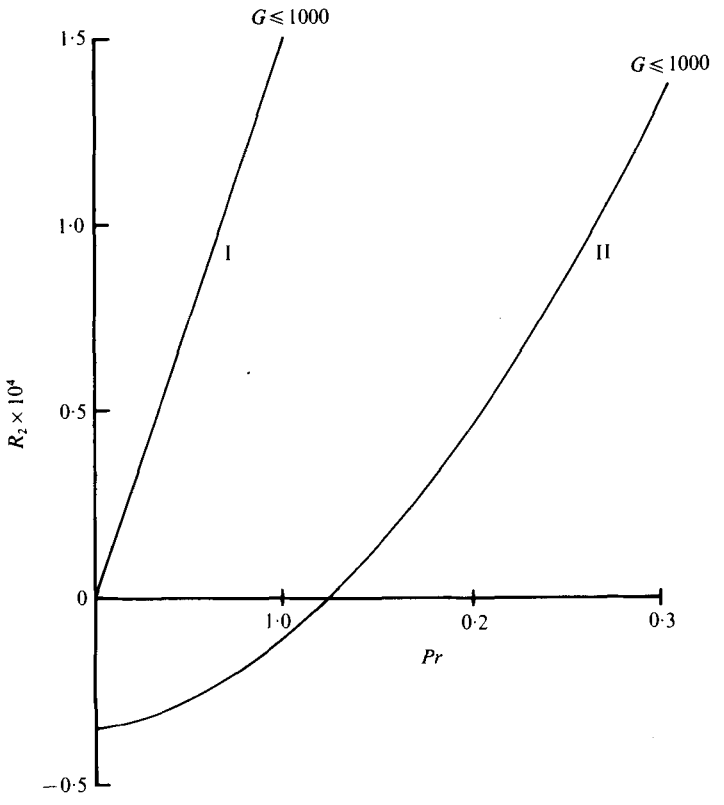

FIGURE 7. $R_2 = (Ra^c - R_0)/G^2$ *vs.* Pr for rigid boundaries and small Prandtl numbers. I, longitudinal steady rolls (even mode); II, transverse steady rolls.

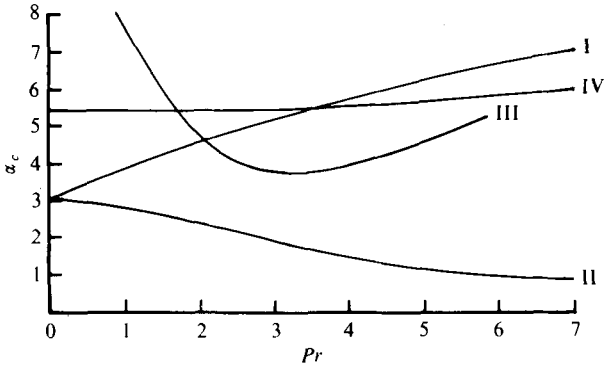

FIGURE 8. Critical wavenumber *vs.* Prandtl number for rigid boundaries and $G = 1000$. Curves as in figure 6.

From the preceding discussion we note that the effect of shear acts in opposite ways for free and rigid boundaries in the limit of small Prandtl numbers. This is obviously due to the different forms of the two basic velocity profiles (2.6) and (2.7). In the free case U_* is very well approximated by a sine profile with half a wavelength between the bounding planes (see I), while for rigid boundaries U_* is close to a sine profile with one full wavelength between the planes. Now it has been shown by Lin (1945), and more

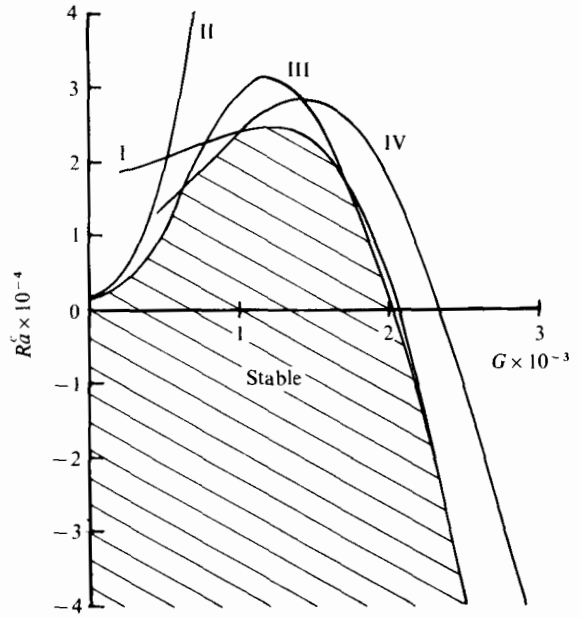

FIGURE 9. Critical Rayleigh number *vs.* Grashof number for $Pr = 6{\cdot}7$ and rigid boundaries. I, longitudinal steady rolls (odd mode); II, transverse steady rolls; III, longitudinal steady rolls (even mode); IV, transverse oscillatory rolls.

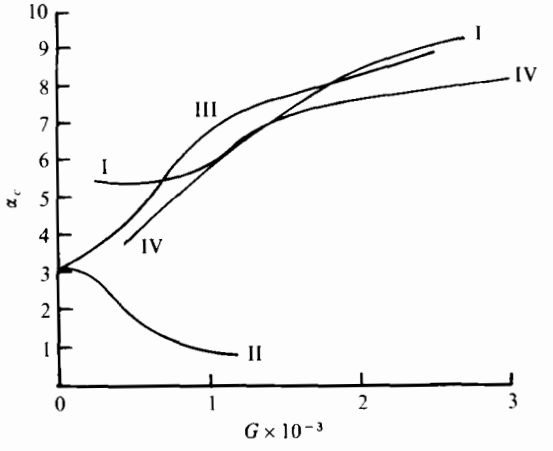

FIGURE 10. Critical wavenumber *vs.* Grashof number for $Pr = 6{\cdot}7$ and rigid boundaries. Curves as in figure 9.

explicitly by Høiland (1953), that an inviscid shear flow with a harmonic velocity profile with less than half its profile wavelength between the planes is stable to transverse infinitesimal disturbances. This is so even though the velocity profile satisfies the Rayleigh–Fjørtoft criterion. Hence a stabilizing tendency should be expected for transverse rolls in the free case and a destabilizing tendency in the rigid case. This should be so particularly in the limit of small Pr, when advection of momentum is increasingly important.

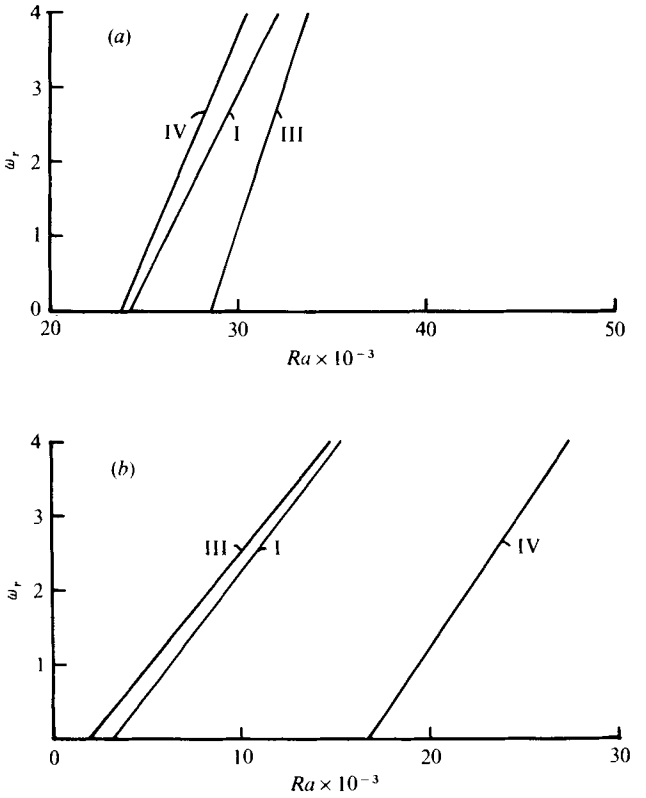

FIGURE 11. Growth rate ω_r *vs.* Rayleigh number for $Pr = 6{\cdot}7$ and rigid boundaries. (*a*) $G = 1000$: I, longitudinal steady rolls (odd), $m = 5{\cdot}9$; III, longitudinal steady rolls (even), $m = 6{\cdot}8$; IV, transverse oscillatory rolls, $k = 5{\cdot}7$. (*b*) $G = 2000$: I, longitudinal steady rolls (odd), $m = 8{\cdot}4$; III, longitudinal steady rolls (even), $m = 8{\cdot}2$; IV, transverse oscillatory rolls, $k = 7{\cdot}6$.

For larger values of G the Prandtl number range containing transverse rolls tends to decrease, as may be seen from figure 6 for $G = 1000$. Up to this value of G oscillatory modes were never found to be the most unstable. We further note that for $Pr \gtrsim 5{\cdot}8$ the odd longitudinal mode is more unstable than the even mode. Calculating the thermal balance (4.5) for the marginally stable odd mode when $Pr = 10$ and $G = 1000$, we find

$$T_1 = 0{\cdot}06, \quad T_2 = 2{\cdot}67, \quad T_3 = 6{\cdot}87, \quad T_4 = -9{\cdot}60. \tag{5.4}$$

The large positive value of T_3 shows that odd modes use very efficiently the unstable regions near the upper and lower boundaries.

From figure 8 we observe that the critical wavenumber for marginally stable longitudinal rolls increases markedly with Pr. For $Pr = 10$ the critical wavenumber for the odd mode is 7·2, i.e. the cell size is less than half that found in ordinary Rayleigh–Bénard convection. This again stresses the importance of the regions near the boundaries in the energy conversion process.

Finally we have performed some computations for rigid boundaries and fixed Prandtl number. We have chosen $Pr = 6{\cdot}7$, which may prove adequate for comparisons with (future) laboratory experiments. The marginal-stability curves and critical wavenumbers have been displayed in figures 9 and 10. We observe from figure 9 that

longitudinal steady rolls are preferred for all G except $600 \lesssim G \lesssim 1000$, where transverse oscillatory rolls occur. In particular we note that for $Ra = 0$, i.e. no uniform heating from below, longitudinal rolls are more unstable than transverse rolls, which is contrary to the results reported by Hart (1972). In appendix B, table 6, eigenvalues and energy balances for slightly unstable disturbances are displayed for $Pr = 6{\cdot}7$. In particular we note that the energy balance for transverse rolls converges rather slowly. This is due to the broad spectrum of the coefficients in the expansions (3.7), which implies that a large number of terms have to be retained. However, errors involved in the matrix manipulations also begin to appear, so there is no point in adding more terms.

For this Prandtl number we find that the lateral advection of heat through the term $T_1 = Pr\, G\langle\overline{u\theta}\rangle$ does not play an important role in the stability problem. When G is small, instability is governed by heating from below, while, at larger G, the vertical temperature gradient associated with the Hadley circulation is the dominating destabilizing effect.

We have also computed some growth rates ω_r for unstable disturbances when $Pr = 6{\cdot}7$ in the rigid case. The results are displayed for $G = 1000$ and $G = 2000$ (figure 11). It is seen from the figures that ω_r is a linear function of Ra in the region considered. Defining $\Delta Ra = Ra - Ra^c$, where Ra^c is the critical Rayleigh number for the particular mode in question, we find that, for $G = 1000$, $\omega_r = 14{\cdot}3\Delta Ra/Ra^c$ for transverse rolls (IV in figure 11*a*), while for $G = 2000$, $\omega_r = 0{\cdot}6\Delta Ra/Ra^c$ for longitudinal rolls (III in figure 11*b*). This should be compared with the result

$$\omega_r = 2{\cdot}6\Delta Ra/Ra^c,$$

which we obtain for the ordinary Rayleigh–Bénard problem ($G = 0$), when $Pr = 6{\cdot}7$ and $\Delta Ra/Ra^c$ is not too large (less than 1, say); see also Finlayson (1972, p. 163).

6. Summary and concluding remarks

We have examined theoretically the stability of a thermally driven parallel flow uniformly heated from below. The earth's rotation has not been taken into account, and the horizontal boundaries have been assumed to be perfect conductors of heat. Numerical computations have been performed for stress-free as well as rigid boundaries.

For free boundaries and relatively small values of the non-dimensional horizontal temperature gradient G the critical Rayleigh number is always larger than that corresponding to convection without shear. When $0{\cdot}04 < Pr < 5{\cdot}2$ transverse rolls minimize the Rayleigh number, i.e. they constitute the preferred mode of disturbance, while longitudinal rolls occur outside this region. These results are consistent with the analytical results reported in I. It may be concluded that a series-expansion solution with G as a 'small' parameter is valid at least up to $G \sim 10$.

For larger values of G oscillatory modes will be the most unstable. Thus for $G = 1000$ longitudinal oscillatory rolls occur when $Pr < 3{\cdot}4$. In particular, the critical Rayleigh number has a local minimum near $Pr = 1$, where $Ra^c < R_0$. In this case the main source of buoyancy is shown to arise from the basic horizontal temperature gradient. When $Pr > 3{\cdot}4$ transverse oscillatory rolls will constitute the most unstable mode, and for $Pr > 4{\cdot}55$ convection will occur even if the layer is heated from the top. It is shown that the vertical temperature distribution associated with the Hadley circulation is responsible for the breakdown of stability in this case.

For rigid boundaries, which is the most relevant case for comparison with laboratory experiments (but not always when applied to the atmosphere or the ocean), we find that transverse rolls are preferred for small Prandtl numbers. This is shown to arise from the fact that shear is destabilizing for small Prandtl numbers in the rigid case. It is found, however, that for both free and rigid boundaries the basic instability mechanism is of thermal origin for the cases considered in this paper.

For sufficiently large values of G instability associated solely with the Hadley circulation will dominate also when the boundaries are rigid as demonstrated by the present calculations for $Pr = 6{\cdot}7$. Other examples are the results obtained by Birikh (1966) for the special case $Pr \equiv 0$ and $Ra \equiv 0$, where the instability is pure shear instability, and by Hart (1972) for $Pr \neq 0$ and $Ra \equiv 0$. In the latter case instability is shown to be of thermal origin when $Pr > 0{\cdot}05$. For the special case $Ra = 0$ and $Pr = 6{\cdot}7$ the present analysis shows that longitudinal rolls are more unstable than transverse rolls, which is contrary to Hart's results. It is hoped that future analysis and/or experiments may help to sort out this discrepancy.

Let us for a moment return to the problem analysed by Birikh (1966). By assuming that $Pr \equiv 0$, i.e. that the fluid is an infinitely good conductor of heat (which might have some relevance to astrophysics, where the effective thermal conductivity is often greatly enhanced by radiation), and also taking $Ra \equiv 0$, buoyancy drops out of the perturbation problem. Accordingly the inclination of the layer to the vertical does not matter. The system of equations (3.1)–(3.3) reduces to the familiar Orr–Sommerfeld equation with a cubic velocity profile. In the rigid case the flow may become unstable when G reaches a certain critical value, as shown by Birikh (1966). The present calculations give $G_c = 7931$ for $k_c = 2{\cdot}69$, which is close to the values 7968 and 2·6 deduced from Birikh's paper.

We have also investigated the analogous problem for free boundaries. A wide range of wavenumbers and G's have been considered, and only eigenvalues with negative real parts were found. This clearly supports the conclusion from inviscid theory in § 5 that the velocity profile U, given by (2.6), is stable.

Finally, we once again emphasize what should be evident by now, namely that even small horizontal temperature gradients introduce new and interesting features into the stability problem of a fluid uniformly heated from below. Since these situations frequently occur in geophysics, the problem is of fundamental importance, although one should keep in mind that the parameters G and Ra (defined with conventional eddy values) in many problems may be very much larger than the values considered here. It is nevertheless hoped that the present investigation will shed some light on a very complicated problem.

This work was initiated while the author was visiting the Department of Applied Mathematics and Theoretical Physics, University of Cambridge (UK) on a NATO-Science Fellowship granted by the Royal Norwegian Council for Scientific and Industrial Research.

Appendix A. Analytical solution for small G and free boundaries

Let the solutions for the free case be expanded in powers of G, which is assumed to be small. The zeroth-order system is then identical with the ordinary Rayleigh–Bénard problem. The first-order system, with the exact expressions for U_* and Θ_*, essentially reduces to a set of coupled ordinary inhomogeneous differential equations with variable coefficients. This system is relatively easily solved analytically by Galerkin's method. The solvability condition for the second-order problem then yields a correction to the critical Rayleigh number Ra^c. We finally obtain

$$\left.\begin{aligned} Ra^c &= \tfrac{27}{4}\pi^4 + G^2 R_2 + O(G^4), \\ k_c &= k_0 + O(G^2), \quad m_c = m_0 + O(G^2), \end{aligned}\right\} \tag{A 1}$$

where

$$R_2 = 10^{-3}\{2{\cdot}75Pr^2 + (0{\cdot}128 + 0{\cdot}156Pr + 0{\cdot}638Pr^2)\,k_0^2 + 3{\cdot}49Pr\,m_0^2\} \tag{A 2}$$

and

$$k_0^2 + m_0^2 = \tfrac{1}{2}\pi^2.$$

On using the fact that the non-dimensional horizontal temperature gradient β in I is by definition given by $Pr\,G/Ra$, inspection of (A 1) shows that the present result obtained with the exact U_* and Θ_* differs very little from the equivalent one in I. It is seen from (A 2) that transverse rolls ($k_0 = \pi/\sqrt{2}$, $m_0 = 0$) are preferred when $0{\cdot}039 < Pr < 5{\cdot}19$, while longitudinal rolls ($k_0 = 0, m_0 = \pi/\sqrt{2}$) occur when $Pr < 0{\cdot}039$ or $Pr > 5{\cdot}19$.

Appendix B. Trial functions and truncation levels

For free conducting boundaries the trial functions in (3.7) were chosen as follows:

$$X_n = Y_n = \begin{cases} \cos n\pi y, & n \text{ odd}, \\ \sin n\pi y, & n \text{ even}, \end{cases} \tag{B 1}$$

$$Z_n = \begin{cases} \sin n\pi y, & n \text{ odd}, \\ \cos n\pi y, & n \text{ even} \quad (=0, 2, 4, \ldots). \end{cases} \tag{B 2}$$

For rigid conducting boundaries we assumed trial functions of the form

$$\left.\begin{aligned} X_n &= V_n y^{n-1}(y^2 - \tfrac{1}{4})^2, \\ Y_n = Z_n &= T_n y^{n-1}(y^2 - \tfrac{1}{4}), \end{aligned}\right\} \quad n = 1, 2, 3, \ldots, \tag{B 3}$$

where V_n and T_n are weighting factors chosen such that

$$\langle X_n^2 \rangle = 1, \quad \langle Y_n^2 \rangle = 1, \tag{B 4}$$

i.e. convergence is associated essentially with the values of the coefficients a_n, b_n and c_n in (3.7).

To indicate truncation levels we have displayed the eigenvalues and energy balance for slightly unstable disturbances when $Pr = 1$ and $Pr = 6{\cdot}7$ in tables 5 and 6.

	N	ω_r	ω_i	$\partial T_0/\partial t$	$T_1+T_2+T_3+T_4$
Free boundaries	2	1·4552	0	0·6128	0·6128
transverse rolls	4	2·3708	0	0·9420	0·9420
$Ra = 9000$	6	2·3708	0	0·9420	0·9420
$k = 0·9$	8	2·3708	0	0·9420	0·9420
	10	2·3708	0	0·9420	0·9420
Free boundaries	1	0·9104	22·9305	0·2276	0·2276
longitudinal	2	0·6439	24·1113	0·1695	0·1695
rolls (even)	3	0·6427	24·1138	0·1667	0·1667
$Ra = 1000$	4	0·6426	24·1139	0·1666	0·1666
$m = 1·4$	5	0·6426	24·1139	0·1666	0·1666
Rigid boundaries	2	2·5168	0	1·6179	1·6179
transverse rolls	4	2·6320	0	1·4614	1·4614
$Ra = 3700$	6	2·6790	0	1·4266	1·4266
$k = 2·9$	8	2·6821	0	1·4197	1·4197
	10	2·6822	0	1·4185	1·4185
	12	2·6822	0	1·4184	1·4184
	14	2·6822	0	1·4184	1·4184
Rigid boundaries	1	5·9592	0	2·9796	2·9796
longitudinal	2	6·2893	0	2·9967	2·9967
rolls (even)	3	6·2702	0	3·0784	3·0784
$Ra = 4300$	4	6·2713	0	3·1080	3·1080
$m = 4$	5	6·2713	0	3·1089	3·1089
	6	6·2713	0	3·1089	3·1089

TABLE 5. Eigenvalues and energy balance (4.5) for $G = 1000$ and $Pr = 1$.

	N	ω_r	ω_i	$\partial T_0/\partial t$	$T_1+T_2+T_3+T_4$
Rigid boundaries	4	0·6305	0	0·1993	0·1993
longitudinal	5	0·8114	0	0·0996	0·0996
rolls (even)	6	0·8045	0	0·1233	0·1233
$Ra = 4500$	7	0·8086	0	0·1576	0·1576
$m = 8·4$	8	0·8086	0	0·1656	0·1656
	9	0·8086	0	0·1468	0·1468
	10	0·8086	0	0·1637	0·1637
	11	0·8086	0	0·1677	0·1677
	12	0·8086	0	0·1677	0·1677
Rigid boundaries	3	0·5886	0	0·2250	0·2250
longitudinal	4	0·4221	0	0·2267	0·2267
rolls (odd)	5	0·4564	0	0·0888	0·0888
$Ra = 4500$	6	0·4583	0	0·0379	0·0379
$m = 8·4$	7	0·4583	0	0·0411	0·0411
	8	0·4583	0	0·0488	0·0488
	9	0·4583	0	0·0521	0·0521
	10	0·4583	0	0·0526	0·0526
	11	0·4583	0	0·0521	0·0521
Rigid boundaries	8	1·1977	107·054	0·7999	0·7999
transverse rolls	10	0·5071	107·744	0·0598	0·0598
$Ra = 18000$	12	0·4916	107·699	0·0123	0·0123
$k = 7·7$	14	0·5036	107·687	0·0092	0·0092
	16	0·5086	107·682	0·0026	0·0026
	18	0·5090	107·682	0·0005	0·0005
	20	0·5090	107·682	0·0002	0·0002
	22	0·5090	107·682	0·0001	0·0001

TABLE 6. Eigenvalues and energy balance (4.5) for $G = 2000$ and $Pr = 6·7$.

REFERENCES

ASAI, T. 1970 Three-dimensional features of thermal convection in a plane Couette flow. *J. Met. Soc. Japan* **48**, 18.

BERKOVSKY, B. M. & FERTMAN, V. E. 1970 Advanced problems of free convection in cavities. *4th Int. Heat-Transfer Conf., France*, vol. 4, p. 12.

BIRIKH, R. V. 1966 On small perturbations of a plane parallel flow with cubic velocity profile. *J. Appl. Math. Mech.* **30**, 432.

CORMACK, D. E., STONE, G. P. & LEAL, L. G. 1975 The effect of upper surface conditions on convection in a shallow cavity with differentially heated end walls. *Int. J. Heat Mass Transfer* **18**, 635.

ELLINGSEN, T. & PALM, E. 1975 Stability of linear flow. *Phys. Fluids* **18**, 487.

FINLAYSON, B. A. 1972 *The Method of Weighted Residuals and Variational Principles.* Academic Press.

GALLAGHER, A. P. & MERCER, A. McD. 1965 On the behavior of small disturbances in plane Couette flow with a temperature gradient. *Proc. Roy. Soc.* A **286**, 117.

GILL, A. E. 1974 A theory of thermal oscillations in liquid metals. *J. Fluid Mech.* **64**, 577.

HART, J. E. 1970 Thermal convection with sloping parallel boundaries. Ph.D. thesis, Dept. of Meteorology, M.I.T.

HART, J. E. 1972 Stability of thin non-rotating Hadley circulations. *J. Atmos. Sci.* **29**, 687.

HURLE, D. T. J., JAKEMAN, E. & JOHNSON, C. P. 1974 Convective temperature oscillations in molten gallium. *J. Fluid Mech.* **64**, 565.

HØILAND, E. 1953 On two-dimensional perturbation of linear flow. *Geofys. Publ.* XVIII, no. 9.

IMBERGER, J. 1974 Natural convection in a shallow cavity with differentially heated end walls. Part 3. Experimental results. *J. Fluid Mech.* **65**, 247.

KELLY, R. E. 1977 The onset and development of Rayleigh–Bénard convection in shear flows: a review. *Proc. Int. Conf. Phys. Chem. Hydrodyn., Oxford* (in Press).

KOSCHMIEDER, E. L. 1966 On convection on a nonuniformly heated plane. *Beitr. Phys. Atmos.* **39**, 208.

LIN, C. C. 1945 On the stability of two-dimensional parallel flows. Part II – Stability in an inviscid fluid. *Quart. Appl. Math.* **3**, 218.

NEUMAN, J. & MAHRER, Y. 1974 A theoretical study of the sea and land breezes of circular islands. *J. Atmos. Sci.* **31**, 2027.

WALSH, J. E. 1974 Sea breeze theory and applications. *J. Atmos. Sci.* **31**, 2012.

WEBER, J. E. 1973 On thermal convection between non-uniformly heated planes. *Int. J. Heat Mass Transfer* **16**, 961.